AMERICAN SOCIETY FOR MICROBIOLOGY | Journal of Bacteriology

GroEL2 of *Mycobacterium tuberculosis* Reveals the Importance of Structural Pliability in Chaperonin Function

Neeraja Chilukoti,[a]* C. M. Santosh Kumar,[b] Shekhar C. Mande[b]

Laboratory of Structural Biology, Centre for DNA Fingerprinting and Diagnostics, Hyderabad, India[a]; Laboratory of Structural Biology, National Centre for Cell Science, Pune, India[b]

ABSTRACT

Intracellular protein folding is mediated by molecular chaperones, the best studied among which are the chaperonins GroEL and GroES. Conformational changes and allosteric transitions between different metastable states are hallmarks of the chaperonin mechanism. These conformational transitions between three structural domains of GroEL are anchored at two hinges. Although hinges are known to be critical for mediating the communication between different domains of GroEL, the relative importance of hinges on GroEL oligomeric assembly, ATPase activity, conformational changes, and functional activity is not fully characterized. We have exploited the inability of *Mycobacterium tuberculosis* GroEL2 to functionally complement an *Escherichia coli groEL* mutant to address the importance of hinge residues in the GroEL mechanism. Various chimeras of *M. tuberculosis* GroEL2 and *E. coli* GroEL allowed us to understand the role of hinges and dissect the consequences of oligomerization and substrate binding capability on conformational transitions. The present study explains the concomitant conformational changes observed with GroEL hinge variants and is best supported by the normal mode analysis.

IMPORTANCE

Conformational changes and allosteric transitions are hallmarks of the chaperonin mechanism. We have exploited the inability of *M. tuberculosis* GroEL2 to functionally complement a strain of *E. coli* in which *groEL* expression is repressed to address the importance of hinges. The significance of conservation at the hinge regions stands out as a prominent feature of the GroEL mechanism in binding to GroES and substrate polypeptides. The hinge residues play a significant role in the chaperonin activity *in vivo* and *in vitro*.

Molecular chaperones are helper proteins, which play essential roles in folding, assembly, and transport of several cellular proteins (1, 2). Chaperonins, a subclass of the molecular chaperones, are homo- or hetero-oligomeric proteins, which carry out the substrate protein folding in a sequestered cavity. One of the best-characterized chaperonins is the 60-kDa chaperonin of *Escherichia coli*, GroEL (3). Chaperonins are highly conserved proteins and are known to interact with nonnative substrate proteins in an ATP-dependent manner. The *E. coli* genome possesses a single copy of *groEL*, arranged in an operonic arrangement with *groES* and expressed under all growth conditions (4). GroEL forms a cylindrical assembly with two heptameric rings and functions in coordination with the heptameric GroES (5–7). Each subunit of GroEL comprises three domains: (i) an equatorial domain (residues 2 to 133 and 409 to 548), which exhibits ATPase activity and participates in intersubunit and interring interactions; (ii) an apical domain (residues 191 to 374), which binds to substrate polypeptide and cochaperonin GroES; and (iii) an intermediate domain (residues 134 to 190 and 375 to 408), which links apical and equatorial domains in sequence and structure and mediates allosteric communication between the two (8, 9). The two rings of GroEL are termed *cis* and *trans* based on their polypeptide or GroES accepting status, respectively.

Structural, biochemical, and genetic studies on the GroEL-GroES system have led to a detailed understanding of its function and mechanism (5–7). Unfolded protein substrates bind the apical domains of the *cis* cavity. Binding of ATP to the equatorial domains in the same ring triggers a large upward conformational transition in the apical domain, which consequently releases the polypeptides into the cavity (10). The upward movement allows GroES binding at the same sites on the apical domain where the polypeptide was bound, thereby allowing the polypeptide folding in a sequestered environment. This essential communication between the two domains is predominantly mediated by the intermediate domain. Subsequently, binding of ATP to the *trans* ring triggers a further conformational change in the *cis* ring, when GroEL releases the *cis* bound GroES, ADP, and the polypeptide in a folded conformation. Taken together, communication between the equatorial and apical domains in the presence of nucleotides elicits essential conformational changes in the latter, which are efficiently communicated by the intermediate domains (10). Such a communication requires rearrangement of the intermediate domain with respect to the equatorial domain and concomitantly

Received 14 October 2015 **Accepted** 5 November 2015

Accepted manuscript posted online 9 November 2015

Citation Chilukoti N, Kumar CMS, Mande SC. 2016. GroEL2 of *Mycobacterium tuberculosis* reveals the importance of structural pliability in chaperonin function. J Bacteriol 198:486–497. doi:10.1128/JB.00844-15.

Editor: J. S. Parkinson

Address correspondence to Shekhar C. Mande, shekhar@nccs.res.in.

* Present address: Neeraja Chilukoti, Biochemistry Lab, TIFR Centre for Interdisciplinary Sciences, Hyderabad, India.

Supplemental material for this article may be found at http://dx.doi.org/10.1128/JB.00844-15.

with the apical domain by virtue of two hinges that exist on either side of the intermediate domain.

The two hinges, hinges 1 and 2, connecting the equatorial and intermediate domains (EI hinge) and connecting the apical and intermediate domains (AI hinge), respectively, have been known to be critical for the chaperonin function and have thus remained highly conserved in evolution. Variations in the hinge residues have been reported to disturb GroEL's three-dimensional (3D) structure (8, 11, 12), assembly (13), substrate/cochaperonin interaction (14–17), and allostery (18–20), thus affecting its overall function (21, 22). Although these studies implicate a role for hinges in various steps of the GroEL mechanism, a unified understanding on the repercussion of hinge variations on GroEL function is lacking. Moreover, the comparative importance of the two hinges is yet unknown. We have taken advantage of the unusual properties of mycobacterial GroELs to address this aspect of the GroEL mechanism.

Mycobacteria are reported to possess multiple copies of GroELs (23, 24). *Mycobacterium tuberculosis* encodes two copies of *groEL*, of which *groEL1* is arranged in an operon with *groES* and is dispensable whereas *groEL2* is located separately on the genome and is indispensable (25, 26). Unusually, *M. tuberculosis* GroELs exist as lower oligomers when the recombinant proteins are purified from *E. coli* (27–29). Intriguingly, biochemical (29), genetic (30), and structural (31, 32) studies demonstrated *M. tuberculosis* GroELs as inefficient chaperones as a consequence of their lower oligomeric status. Yet abundance of GroEL2 by means of enhanced expression or by chemical collocation has been shown to recover *in vivo* and *in vitro* function (33). Therefore, GroEL2 might be a naturally stunted chaperone, which can function as a canonical chaperonin when present in higher concentrations. Its reduced chaperonin activity is likely to arise either out of weakened substrate interactions, out of impaired stability of the functional oligomeric form, or out of potential defects in allostery. These three important components of chaperonin function can be studied using the mycobacterial chaperonins as a model system. To address this, we have created chimeras of *M. tuberculosis* GroEL2 and *E. coli* GroEL by mutually exchanging either apical or equatorial domains. Since the hinge residues in *E. coli* GroEL and *M. tuberculosis* GroEL2 are largely conserved, in order to understand their role in impairing GroEL2 activity, the domain boundaries in the resulting chimeras were also altered to study the influence of domain boundaries and hinge residues in chaperonin function. Investigating the genetic and biochemical features of these chaperonin variants revealed that mutations at the hinge regions lead to loss of function in spite of substrate binding.

MATERIALS AND METHODS

Materials, plasmids, bacterial strains, and growth conditions. All chemicals and antibiotics were from Sigma, Inc. Restriction enzymes, T4DNA ligase and Phusion polymerase were purchased from New England BioLabs Inc., USA. All the gene amplification reactions were performed with Phusion polymerase (NEB). Antibodies IT13 and IT56 were procured via an NIH-NIAID TB Vaccine Testing and Research Materials contract awarded to Colorado State University, and antibody recognizing *E. coli* GroEL was purchased from Sigma-Aldrich, Inc. The anti-mouse and anti-rabbit secondary antibodies were purchased from Santacruz Biotechnology, Inc. Plasmids used in this study are pET28a (+) (Novagen, Inc., USA), pBAD24 (34), and pSCM1601 and pSCM1603 (30). *E. coli* BL21(DE3), used for overexpression, was cultured in standard LB medium with appropriate antibiotic supplements. *E. coli* LG6, used for *in vivo* complementation studies, was a kind gift from Arthur Horwich and is a derivative of strain MG1655, wherein the chromosomal *groESL* operon is placed downstream to the isopropyl-β-D-thiogalactopyranoside (IPTG)-inducible P_{lac} promoter (35). Plasmids and oligonucleotides used in the study are listed in Tables S1 and S2, respectively, in the supplemental material.

Cloning of *M. tuberculosis groEL2* for complementation studies. *M. tuberculosis groES* and *groEL2* were cloned in pBAD24 in an operonic arrangement with duplicated ribosome binding sites (RBS) placed upstream to both the open reading frames (ORFs) and labeled *M. tuberculosis groEL2*$_{High}$(pSCM2802). In contrast, the construct pSCM1603 (30), labeled *M. tuberculosis groEL2*$_{Low}$, is different in that the RBS upstream from ORFs *groES* and *groEL* were sourced from pBAD24 and pET28a (+), respectively (Fig. 1A).

Construction and cloning of chimeric GroEL variants. All the molecular biology methods were adapted as described earlier (36). The equatorial domains of *M. tuberculosis groEL2* and *E. coli groEL* were mutually exchanged using overlap extension PCR (37) to generate the ORFs *EAI2* and *MAI2*. Likewise, mutual exchange of apical domains generated the ORFs *EA2* and *MA2*. The domain boundaries were altered for probing the role of interdomain flexibility in the four constructs to generate four new ORFs, *EAI1*, *MAI1*, *EA1*, and *MA1*.

The *groEL* variants *EAI2*, *EAI1*, *MAI2*, *MAI1*, *EA2*, *EA1*, *MA2*, and *MA1* were amplified and ligated to EcoRI and HindIII sites of pBAD24, resulting in plasmids pSCM2823, pSCM2822, pSCM2829, pSCM2828, pSCM2811, pSCM2810, pSCM2817, and pSCM2816, respectively (see Table S1 in the supplemental material). Into these plasmids, *M. tuberculosis groES* was ligated in NheI and EcoRI sites, and the resulting plasmids were designated pSCM2819, pSCM2818, pSCM2825, pSCM2824, pSCM2807, pSCM2806, pSCM2813, and pSCM2812, respectively (see Table S1 in the supplemental material). Likewise, *E. coli groES* was ligated to generate the plasmids pSCM2821, pSCM2820, pSCM2827, pSCM2826, pSCM2809, pSCM2808, pSCM2815, and pSCM2814, respectively (see Table S1 in the supplemental material). pSCM2838 was generated by replacing the glycine residue with phenylalanine at position 133 of *EAI1*. The generated chimeras were cloned into pET28a (+) for protein purification.

***In vivo* complementation assay of GroEL variants.** The ability of GroEL variants to complement *E. coli* GroEL was assessed using *E. coli* LG6 as described previously (30). Briefly, stationary-phase cultures of *E. coli* strain LG6 containing plasmids pSCM1601, pSCM1603, pSCM2802, pSCM2803, and pBAD24 were serially diluted and spotted onto LB agar supplemented with either 1 mM IPTG (to induce the chromosomal copy of *E. coli groES-groEL*) or 0.2% D-glucose (to repress the P_{BAD} promoter) or 0.2% L-arabinose (to induce the expression of cloned *groEL* variants). A similar method was adapted for *groEL* variants generated in this study to assess their complementation ability.

Immunoblotting to detect the expression of cloned genes in *E. coli* LG6. *E. coli* LG6 strains expressing *groEL* variants were grown in LB supplemented with 0.2% L-arabinose and 1 mM IPTG and were recovered in mid-log phase. The resultant lysates were resolved on either 10% SDS-PAGE for checking expression levels or 6% native PAGE for checking oligomeric status and transferred to a polyvinylidene difluoride (PVDF) membrane (Millipore). Contingent to the GroEL variants resolved, the membranes were probed with two different *M. tuberculosis* GroEL2-specific antibodies: IT56, which recognizes the GroEL2 equatorial domain, or IT13, which recognizes the apical domain at a dilution of 1:2,000. The blot was developed using the ECL Western blotting detection kit (GE Biosciences).

Protein purification. The protocol for purification of *E. coli* GroEL and *M. tuberculosis* GroEL2 was carried out as described previously (30, 31). The recombinant GroEL variants were expressed in *E. coli* BL21(DE3) with 0.5 mM IPTG at 18°C for 16 h. The cells were lysed and subjected to ammonium sulfate extraction. All the chimeras were salted in at 15% and salted out at 30%. The salted-out proteins were suspended in a buffer

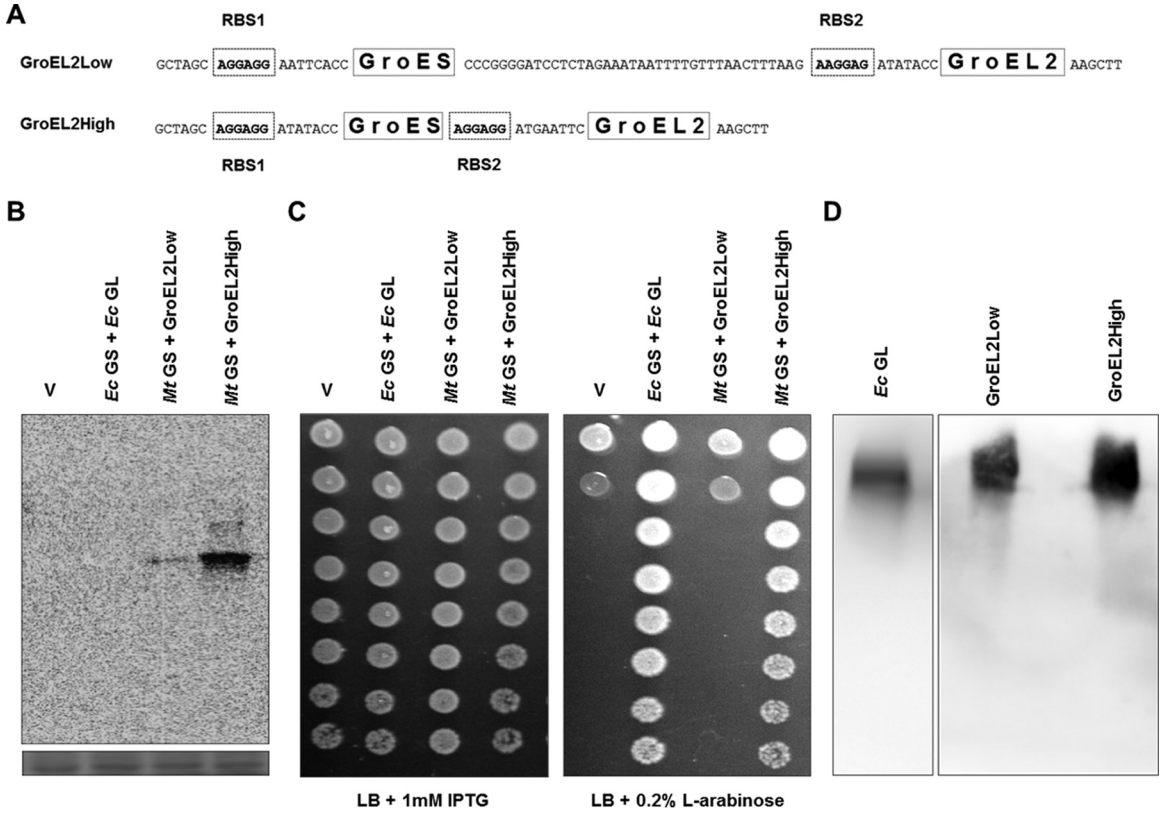

FIG 1 *M. tuberculosis* GroEL2 can complement *E. coli* GroEL only upon high levels of overexpression. (A) Schematic representation of the GroEL2High and GroEL2Low constructs showing the RBS and sequence difference between *groES* and *groEL2* in pBAD24. (B) The cultures of *E. coli* LG6 harboring plasmids pSCM1601, pSCM1603, pSCM2802, and pBAD24 were grown to mid-log phase in the presence of 0.2% L-arabinose and 1 mM IPTG. The cell lysates were resolved on 10% SDS-PAGE or native PAGE, transferred, and probed with *M. tuberculosis* GroEL2-specific antibody. Ponceau-stained membranes were placed below the respective immunoblots, showing equal loading of the total cell protein from indicated GroEL2 variants. (C) The log-phase cultures of *E. coli* LG6 producing the indicated GroELs were serially diluted and spotted onto LB agar plates supplemented as indicated. The plates were incubated at 30°C. (D) Lysates of cultures of *E. coli* LG6 expressing GroEL2Low and GroEL2High were resolved on 6% native PAGE and probed with antibodies specific to *M. tuberculosis* GroEL2 and *E. coli* GroEL.

containing 50 mM Tris-HCl (pH 8.0) and 1 mM EDTA using PD-10 columns (GE Biosciences). The protein sample was loaded on Q Sepharose (GE Biosciences), and the GroEL variants were eluted using a buffer consisting of 150 mM NaCl, 50 mM Tris-HCl (pH 8.0), and 1 mM EDTA. The proteins were buffer exchanged and concentrated using Amicon concentrators in 10 mM Tris-HCl (pH 8.0) for further use.

Gel filtration chromatography to analyze the oligomeric status of the GroEL chimeras. GroEL variants (500 μg) were resolved on HiPrep 16/60 Sephacryl S-300 HR at a flow rate of 0.5 ml/min. The absorbance at 280 nm was recorded for elution to estimate the oligomerization status of these variants.

Normal mode analysis of *M. tuberculosis* GroEL2. Since *M. tuberculosis* GroEL2 crystal structures lack the N-terminal 61 residues and GroEL2 is depicted in a single conformation (31), we have modeled GroEL2 using the *E. coli* GroEL structure in two individual conformations, the R and T states. The *M. tuberculosis* GroEL2 sequence was modeled using the coordinates from the *E. coli* GroEL structure (PDB 1AON) for the chains A and H, which represent the R and T conformations. Five models were generated for each conformation using Modeller 9.13 (38), and the model with the lowest energy was selected. Likewise, models were generated for the eight chimeras. C-terminal residues in the models were disordered since the homologous region in *E. coli* GroEL is not resolved (8). Therefore, coordinates for the unstructured residues homologous to the 21 C-terminal residues of *E. coli* GroEL were removed prior to normal mode analysis. Transitions between the two states for individual GroEL variants were generated by calculating the contribution of each normal mode to the observed conformational change using Elastic Network Model (39). The individual normal modes and their deformations were visualized using Pymol 1.3.

RESULTS

Mycobacterial GroEL2 can functionally replace *E. coli* GroEL upon enhanced expression. The two *groEL2* constructs $groEL2_{Low}$ and $groEL2_{High}$ differ in ribosome binding sites upstream of the *groEL2* ORF (Fig. 1A) but intriguingly lead to a significant difference in the levels of proteins expressed (Fig. 1B), although expression of both genes is under the arabinose-inducible P_{BAD} promoter. The precise reason for such differences in GroEL2 expression is unclear. This difference in expression might be due to a larger spacer between the stop codon of *groES* and the RBS of *groEL2* for GroEL2Low compared to GroEL2High. However, this system gave an interesting model to test the complementation ability of *M. tuberculosis* GroEL2. Earlier complementation studies reported that at higher levels of expression, *M. tuberculosis* GroEL2 can functionally replace *E. coli* GroEL, but at lower levels of expression it is unable to do so (30, 33). We therefore transformed *E. coli* LG6 with the plasmid vectors pSCM1603 and pSCM2802 that harbor $groEL2_{Low}$ and $groEL2_{High}$, respectively, in

operonic arrangement with the cognate *M. tuberculosis groES*. Functional replacement of *E. coli* GroEL by GroEL2High indicates that at higher levels of expression *M. tuberculosis groEL2* can support growth of *E. coli* LG6 (Fig. 1C). Since hydrophobicity drives the GroEL-substrate protein interactions, complementation by overexpression could be due to the accumulation of a greater number of hydrophobic patches in GroEL2High contributing to an avidity effect or due to the GroEL2 molecules making a functional chaperonin. To probe these possibilities, we attempted to understand the oligomeric status of GroEL2 in these two strains by resolving the lysates through native PAGE followed by Western blotting with GroEL2-specific IT56 antibody. Interestingly, the oligomeric status of GroEL2 was seen to be similar in GroEL2Low and GroEL2High (Fig. 1D), suggesting that the activity exhibited by GroEL2High is due to the avidity effect. However, a comprehensive understanding of the functional and structural features of GroEL2High and GroEL2Low is needed to learn the intricate features of this behavior. Our observation raises the interesting possibility that GroEL2 is an impaired chaperone that is able to match the activity of a fully effective chaperone only upon abundance. GroEL2 of *M. tuberculosis* therefore presents an interesting system to probe different aspects of chaperonin function.

Our earlier study with *M. tuberculosis* GroEL1 had suggested that GroEL1 could complement only upon facilitated oligomerization. The facilitation would be mediated by mutual exchange of the oligomerizing equatorial domains between *E. coli* and *M. tuberculosis* chaperonins (30). However, the inability of *M. tuberculosis* GroEL2 to functionally replace *E. coli* GroEL has been intriguing. Interestingly, multiple-sequence alignments of mycobacterial sequences have suggested variations at the interdomain boundaries in *M. tuberculosis* GroEL2 (31), which probably interfere with the interdomain allostery and thereby the overall activity of the chaperonins. We therefore attempted to generate chimeras of *M. tuberculosis* GroEL2 and *E. coli* GroEL by exchanging equatorial and apical domains. However, during this process, we realized that the hinge regions between different domains would be affected in making these chimeras. While hinges 1b and 2b are conserved between *E. coli* GroEL and *M. tuberculosis* GroEL2, hinges 1a and 2a are different. Therefore, we also introduced mutations at the hinge residue positions.

Domain-swapping scheme. The hinge regions in GroEL have been demonstrated to mediate interdomain movements (Fig. 2A and B) (40). Sequence comparison of *E. coli* GroEL and *M. tuberculosis* GroEL2 revealed variations at the hinge residues (Fig. 2B). Since these chaperonins are functionally identical *in vivo* (Fig. 1C), the said variations present an interesting opportunity to probe the role of hinge residues. We therefore created domain-exchanged GroEL chimeras using the ORFs of *E. coli* GroEL and *M. tuberculosis* GroEL2. Into these chimeras, hinge residues were modified to match those in either of the wild-type GroELs to additionally generate chimeras with point mutations at the hinges (Fig. 2B). These chimeras were probed using genetic, biochemical, and computational tools to present a comprehensive picture on the significance of hinge regions in the mechanism of GroEL.

Mutual exchange of equatorial domains resulted in chimeras EAI2 and MAI2, while exchange of apical domains resulted in chimeras EA2 and MA2 (Fig. 2B and C). In the chimera designations, A, I, and E represent the apical, intermediate, and equatorial domains, respectively, while E and M represent the domain sources *E. coli* GroEL and *M. tuberculosis* GroEL2, respectively. The numbers 1 and 2 represent different GroEL variants with the same combination of domains. For example, EA2 is a chimera with the apical domain of *E. coli* GroEL and the equatorial and intermediate domains from *M. tuberculosis* GroEL2. Furthermore, hinge regions were altered in the above chimeras as following. Variations were introduced at hinge 1 for EAI1 (::Gly at hinge 1a and ΔGlu-Gly pair at hinge 1b) and MAI1 (ΔGly at hinge 1a and ::Glu-Gly pair at hinge 1b). Similarly, mutations were incorporated at hinge 2 for EA1 (::Glu-Gly pair at hinge 2a and ΔVal-Ala pair at hinge 2b) and MA1 (ΔGlu-Gly pair at hinge 2a and ::Val-Ala pair at hinge 2b). These chimeras were cloned under the arabinose-inducible P_{BAD} promoter along with *E. coli* or *M. tuberculosis groES*. Genetic studies in *E. coli* LG6 followed by biochemical studies with purified proteins presented a comprehensive understanding of these GroEL variants *in vivo* and *in vitro*.

Pliability at two hinges has differential effects on GroEL function. The activity of chimeric variants of *E. coli* GroEL and *M. tuberculosis* GroEL2 with equatorial domain exchange was first assayed in *E. coli* LG6. Chimeras with the equatorial domain of *M. tuberculosis* GroEL2, EAI1 and EAI2, exhibited complex behavior. While EAI1 could function with either of the two GroES homologs in rescuing *E. coli* LG6, EAI2 showed moderate activity only in the presence of *E. coli* GroES (Fig. 3A). It is interesting that EAI1 has an insertion of a Gly at hinge 1a and deletion of Glu-Gly at hinge 1b. EAI2, on the other hand, possesses an Ala-to-Lys mutation at hinge 1a due to the swapping of domains. As these chimeras bear the apical domain of *E. coli* GroEL, it might be assumed that EAI2's lack of complementation with *M. tuberculosis* GroES but weak complementation with *E. coli* GroES is due to recognition of its cognate *E. coli* GroES. *M. tuberculosis* and *E. coli* GroES are homologous, with 43% identity with a few modifications at the GroEL interacting mobile loop. While *E. coli* GroES has the characteristic IVL sequence at the tip of the mobile loop, that in *M. tuberculosis* GroES is reversed to LVI. Similarly, the tip of the mobile loop in *E. coli* GroES is surrounded by smaller residues, whereas that in *M. tuberculosis* GroES is surrounded by the bulkier residues Leu and Pro, indicating possible differences in the interactions with GroEL.

Chimeras bearing the equatorial domain of *E. coli* GroEL, MAI1 and MAI2, were fully active (Fig. 3A). Interestingly, hinge 1a hosts evolutionarily conserved smaller residues (Gly or Ala) between the bulkier residues Lys and Leu, which might impart flexibility for hinge motion (Fig. 2B). Lack of flexibility at hinge 1a in EAI2 could potentially explain its reduced activity (Fig. 2B and 3A). We then addressed the stringency of sequence variations at hinge 2. Interestingly, the four constructs differed with each other in their behavior. EA2, bearing the apical domain of *E. coli* GroEL, displayed significant activity in the presence of *M. tuberculosis* GroES and moderate activity in the presence of *E. coli* GroES, whereas MA2 displayed weak or no activity (Fig. 4A). Neither of the chimeras with indels at hinge 2, EA1 or MA1, was seen to be functional (Fig. 4A). These results clearly indicate that hinge 2 is far less accommodative of variations, unlike hinge 1. Hinge 2 is responsible for essential extensive conformational transitions and leads to an ~60° upward rotation followed by an ~90° clockwise twist of the apical domain along the long axis. Consequently, variations at hinge 2 would lessen the flexibility and thereby hamper the mobility of the apical domain and overall function of the chaperonins. Therefore, hinge 2 appears to be less accommodative of the mutations, especially for the bulkier residues. Interestingly,

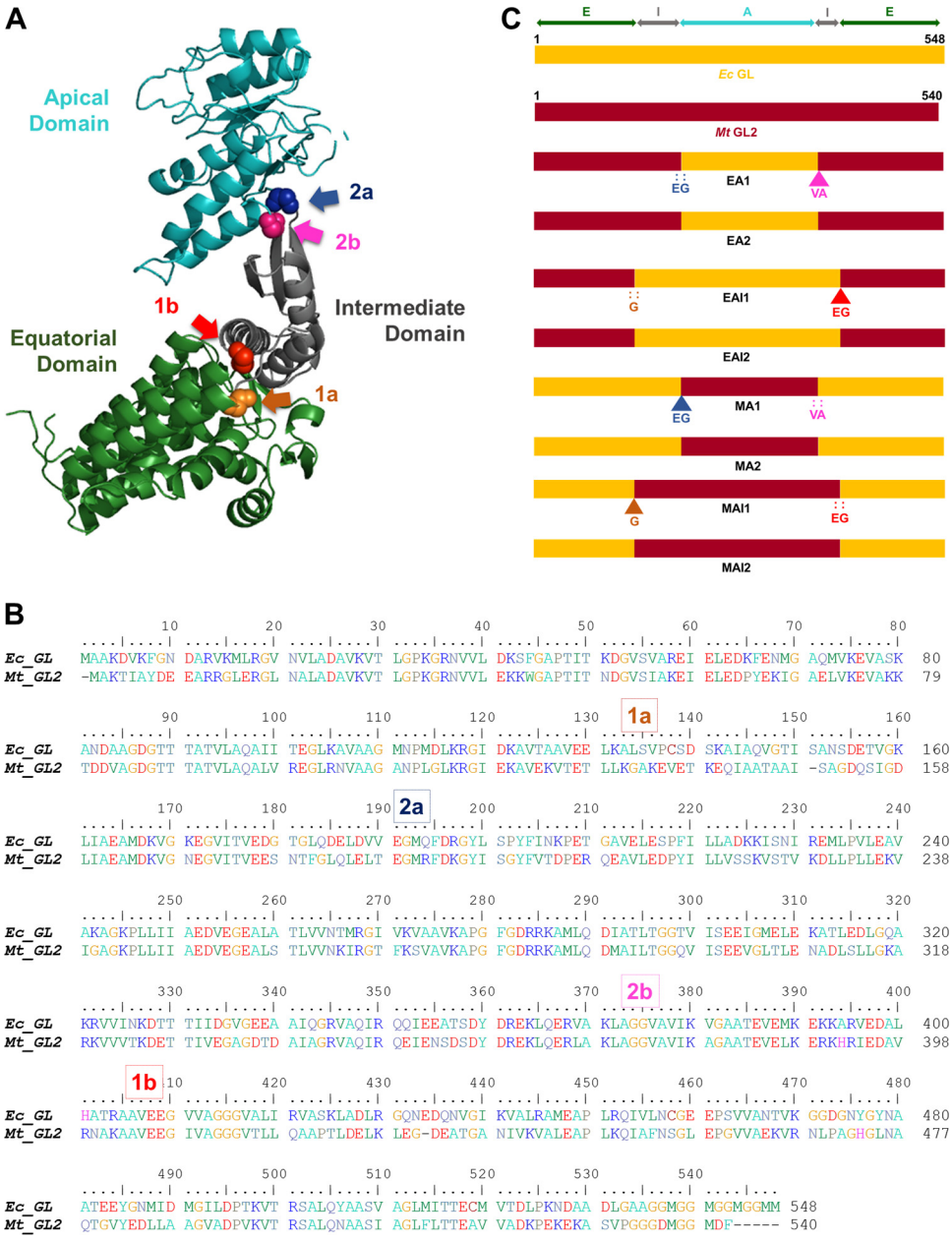

FIG 2 Interdomain hinges in GroEL are conserved. (A) Ribbon diagram of the GroEL monomer with residues at the interdomain hinges shown as spheres. (B) Sequence alignment of *E. coli* GroEL and *M. tuberculosis* GroEL2. Arrows indicate the hinge regions. Alignment was performed using BioEdit 7.2.5. The sequences are shaded with a color code depicting the individual domains as in panel A, and the positions of hinge regions that were probed in this study are indicated. (C) Schematic representation of domain allocation in the indicated GroEL chimeras. Regions spanning the equatorial (E), intermediate (I), and apical (A) domains are color coded as in the cartoon. Indicated insertions (::) and deletions (Δ) are color coded to the regions on the cartoon and in the alignment.

the immunoblots showing expression of these chimeras indicate similar amounts of each chimera in the presence or absence of cochaperonin, suggesting that the complementation ability of the chimeras is due to their intrinsic behavior (Fig. 3B and 4B).

Intrigued by the presence of glycine in EAI1 at hinge 1a, we wished to understand the role of glycine at this hinge. We therefore substituted a bulkier phenylalanine at this position. Surprisingly, the resulting mutation did not affect the chaperone activity (Fig. 3C), implying that hinge 1 can accommodate bulkier residues. Taken together, these results indicate that hinge 2 is critical in chaperonin action *in vivo* while hinge 1 is more accommodative.

GroEL variants inherited their parental behavior to determine oligomeric assembly. Having established that the hinge variations affect chaperonin function *in vivo*, we wished to understand if the observed variations in activity were a consequence of impaired chaperonin oligomeric assembly. The GroEL variants were purified with ammonium sulfate fractionation followed by ion-exchange chromatography. The purified proteins were resolved on Sephacryl S-300 to study their oligomeric status. The

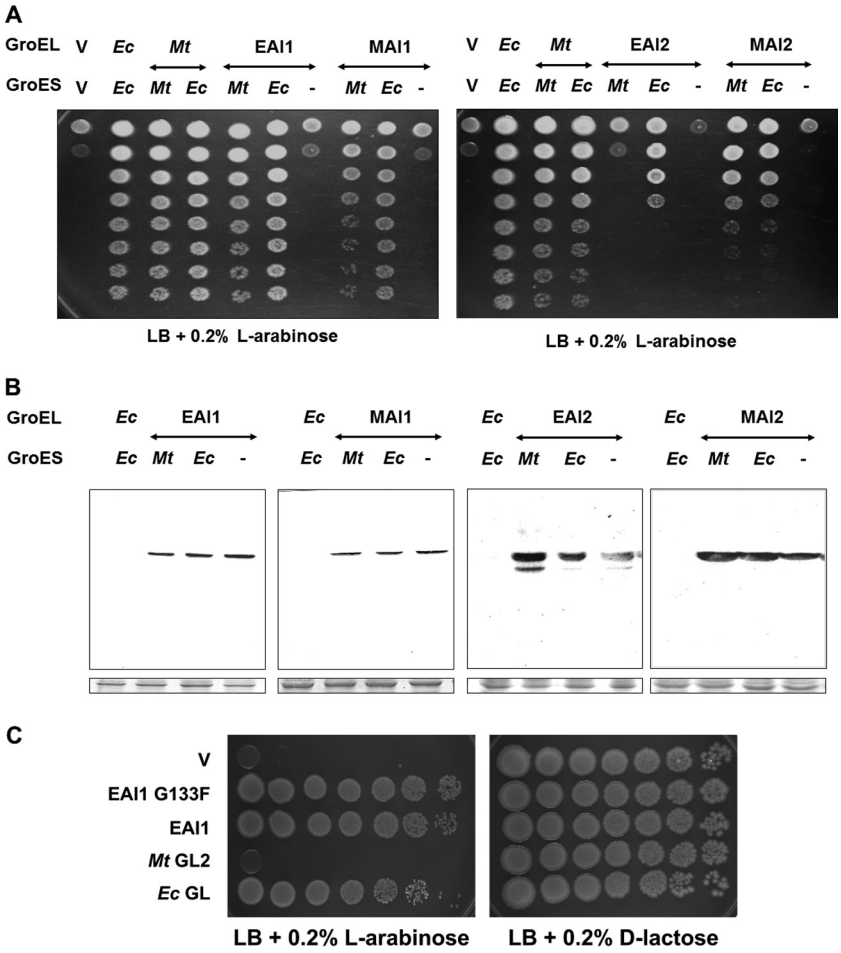

FIG 3 Complementation analysis of the constructs obtained by equatorial domain swapping. (A) Log-phase cultures of *E. coli* LG6 expressing the indicated chaperonins were serially diluted and spotted onto LB agar plates supplemented with 0.2% L-arabinose. The plates were incubated at 30°C. (B) The cultures were grown until mid-log phase in LB supplemented with 0.2% L-arabinose and 1 mM IPTG. Cell lysates were resolved on 10% SDS-PAGE and probed with GroEL2-specific antibody. The panels below the immunoblots show Ponceau-stained membranes as loading control. (C) Log-phase cultures of *E. coli* LG6 expressing the indicated chaperonins were serially diluted and spotted onto LB agar plates supplemented with either 0.2% L-arabinose or 0.2% D-lactose. The plates were incubated at 30°C.

chromatograms revealed that all the chimeras existed as tetradecamers, although lower oligomeric species were observed for three chimeras. Chimeras with mycobacterial equatorial domain EAI2 and EA2 displayed distinct tetradecameric form. The respective hinge variant versions EAI1 and EA1 existed in equilibrium between a tetradecamer and a dimer, a feature reminiscent of the parent *M. tuberculosis* GroEL2 (29, 41). Interestingly, EAI1and EA2 were able to effectively rescue *E. coli* LG6, but EAI2 and EA1 failed to complement, suggesting that these chaperonin variants might be similar to *M. tuberculosis* GroEL2, wherein oligomeric assembly upon their abundance was required to rescue *E. coli* LG6 (Fig. 5).

The chimeras bearing the equatorial domain of *E. coli* GroEL, MAI2 and its variant MAI1, existed as a stable tetradecamer and were able to complement *in vivo*. On the other hand, among chimeras bearing the apical domain of *M. tuberculosis* GroEL2, MA2 exhibited equilibrium between the heptameric and the tetradecameric form and showed complementation whereas MA1, despite existing as a tetradecamer, could not rescue *E. coli* LG6 (Fig. 5). These results clearly suggest that the variations in the hinge regions contribute to the chaperonin function but not the oligomeric assembly.

Parental apical domains drive the substrate interactions of GroEL variants. Substrate interaction and encapsulation drive chaperonin function in an ATP-dependent manner. GroEL binds exposed hydrophobic surfaces on the substrate protein followed by encapsulation in the cavity for folding. We assessed the substrate binding ability of the chimeras in preventing the aggregation of the heat-denatured model substrate porcine citrate synthase (CS). A 365 nM concentration of CS was mixed with the GroEL variants in 1:1, 1:2, and 1:3 molar ratios, and the aggregation was monitored by light scattering as a function of time.

The wild-type chaperonins *M. tuberculosis* GroEL2 (29) and *E. coli* GroEL (30) displayed conventional behavior, and the chimeras displayed activity in between the parents' activity (see Fig. S2A in the supplemental material). However, the behavior of certain chimeras is notable. While the phenotypically active chimera EA2 failed to prevent substrate aggregation, the phenotypically inactive MA1 could readily prevent aggregation of the substrate. On the other hand, the variants of EA2 (EA1) displayed moderately

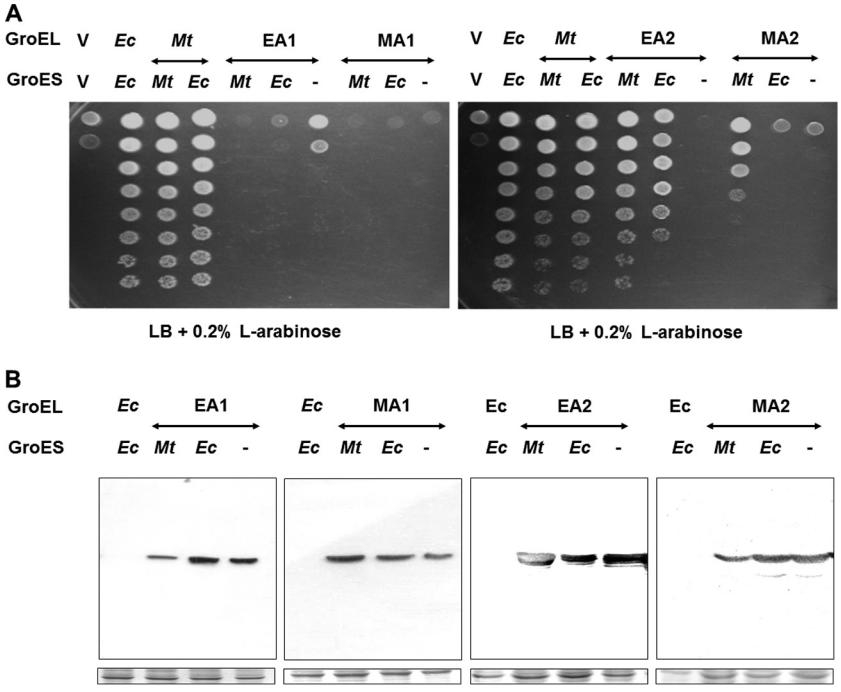

FIG 4 Complementation analysis of the constructs obtained by apical domain swapping. (A) Log-phase cultures of *E. coli* LG6 expressing the indicated chaperonin variants were serially diluted and spotted onto LB agar plates supplemented with 0.2% L-arabinose. The plates were incubated at 30°C. (B) Cultures of LG6 as described for panel A were grown until mid-log phase in LB supplemented with 0.2% L-arabinose and 1 mM IPTG. Cell lysates were resolved on 10% SDS-PAGE, transferred, and probed with GroEL2-specific antibody. Loading controls were represented by respective Ponceau-stained membranes below the immunoblots.

altered behavior. Moreover, such a behavior was observed with different GroEL/CS ratios as well (see Fig. S2A in the supplemental material). While MAI2 and EAI2 showed increased prevention as a function of concentration, the mutant versions MAI1 and EAI1 showed decreased prevention under identical conditions (see Fig. S2A in the supplemental material).

To test if the differences in prevention of substrate aggregation by GroEL variants were not due to inherent instability of the GroEL variants themselves, the heat stability of the GroEL variants was assessed. Individual chimeras were incubated at the three concentrations as described above at 43°C, and their aggregation was monitored. All the chimeras showed aggregation upon increase in the concentration (data not shown). However, all the chimeras exhibited similar CD spectra at 25, 37, and 43°C, suggesting that their secondary structure composition remains similar at 43°C (see Fig. S2B in the supplemental material). These results indicate that although substrate recognition is the fundamental property of the chaperonin, interdomain communication plays an equivalent role in properly orienting and moving the apical domain for substrate recognition and folding.

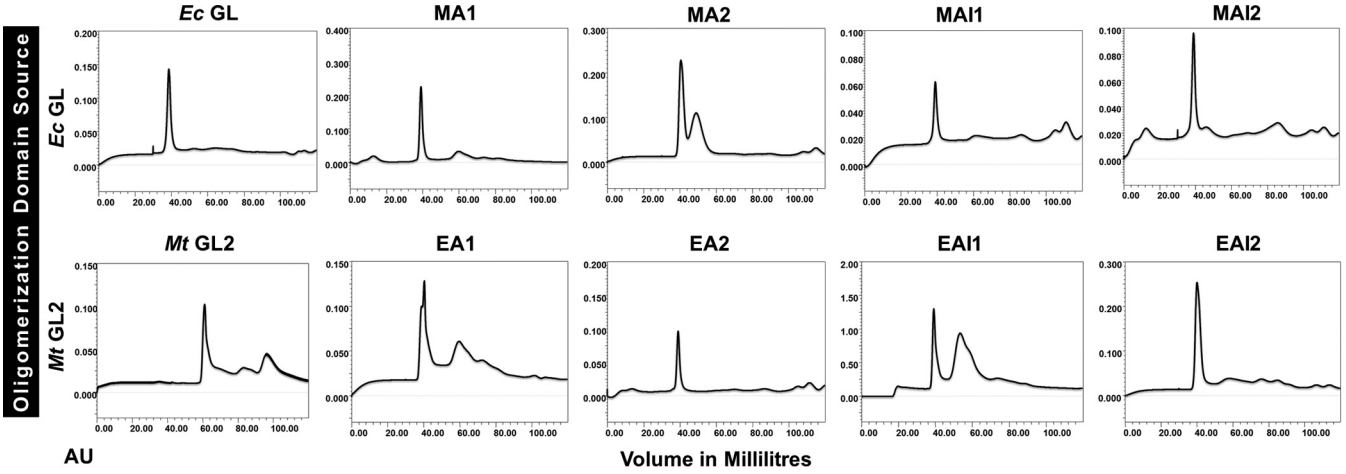

FIG 5 Oligomerization of GroEL variants. The indicated proteins were resolved on Sephacryl S-300 16/60 (GE Biosciences) in a Biologic Duo Flow Fast Performance liquid chromatography system (Bio-Rad) at a flow rate of 0.5 ml/min. AU, absorbance units at 280 nm. The peak at 41 ml corresponds to a tetradecamer.

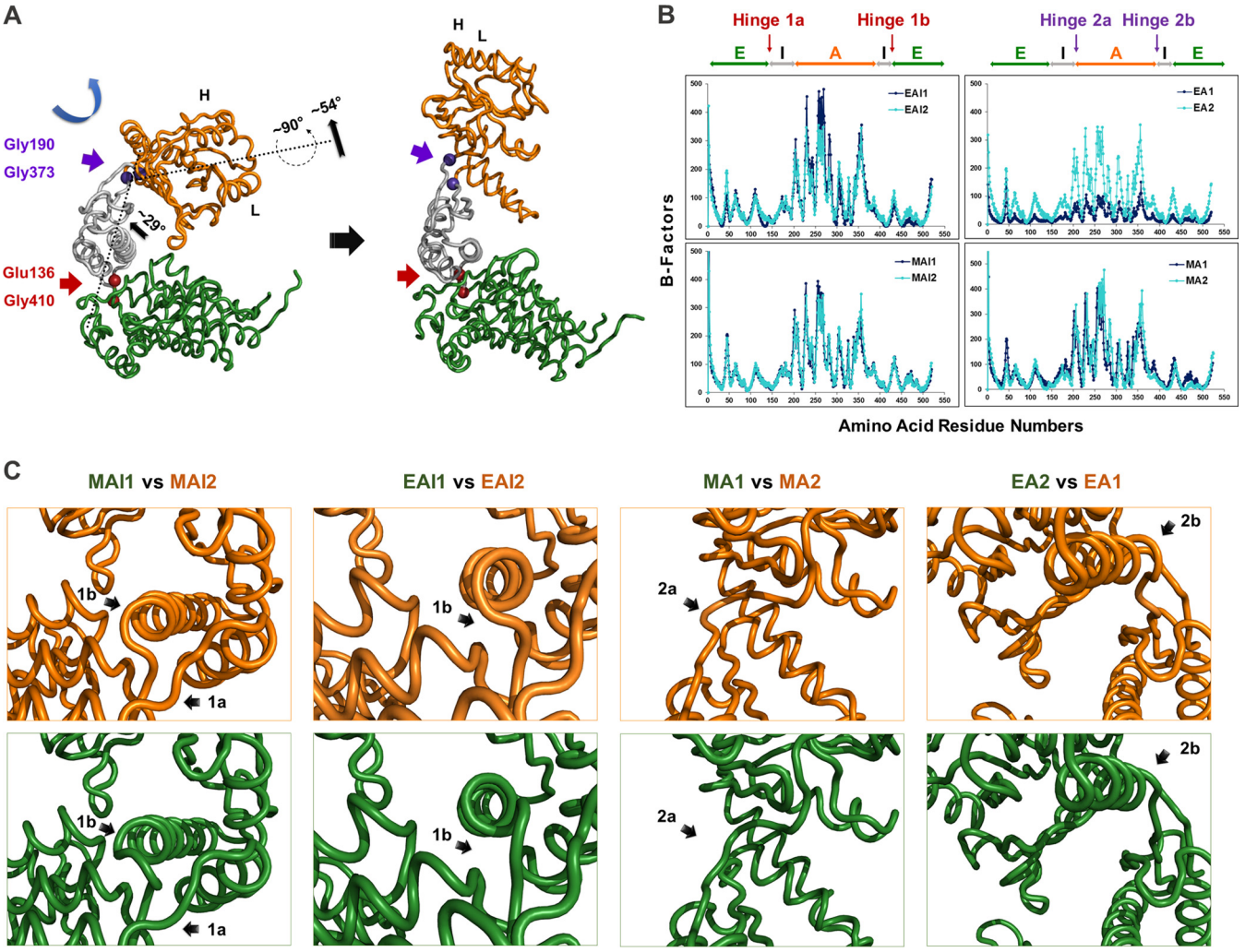

FIG 6 Normal mode analysis depicts steric hindrance to interdomain communication. (A) *M. tuberculosis* GroEL2 sequence was modeled using Modeller 9.13. The model was generated on the extended and compressed conformations of *E. coli* GroEL using the coordinates from PDB (PDB 1AON) for chains A and H, respectively. Transitions between the two conformations were mapped using Elastic Network Model. The alpha carbon traces in the resulted frames were connected in Pymol 1.3. The cartoon represents the resulting initial and final modes. Apical, intermediate, and equatorial domains are color coded in gold, silver, and green, respectively, while the indicated residues at hinges are shown as spheres and color coded in maroon and purple for EI and AI hinges, respectively. Dotted lines indicate the rotational and translational motions that result in the displacement of the substrate binding helices H and L. (B) Comparison of fluctuations in the B-factors of the C^{α} atoms between the indicated GroEL variants, plotted as a function of residue numbers. B-factors describe the displacement of atomic positions in a 3D structure between different conformations of a protein. Regions spanning apical (A), intermediate (I), and equatorial (E) domains on the GroEL structure and the hinge regions are color coded according to the molecular model. (C) The effects of the indels in the indicated GroEL variants are highlighted. The illustrations were generated using Pymol 1.3.

Normal mode analysis depicts constrained domain interfaces that restrict sequence variations. Since residues in the interdomain interface have been shown to regulate the function of GroEL (Fig. 2 to 4), we sought to understand their role in modulating interdomain communication and resulting motion. The three-domain architecture of the GroEL protomer principally adopts two conformations: polypeptide-accepting T state and nucleotide-bound R″ state. The T and R″ conformations are observed in *trans* and *cis* rings in the GroES-GroEL complex (42). Transition between the two conformations essentially involves communication between the equatorial domain (E) and apical domain (A) in response to the presence of nucleotide. Furthermore, the intermediate domain (I) that connects the said domains plays a pivotal role in mediating the communications via conserved interdomain (EI and AI) boundaries, which act as hinges in facilitating the transitions. Therefore, flexibility at the hinges is essential in mediating the domain motions and thereby the overall function. Consequently, aberrations at the hinges have been demonstrated to affect GroEL function adversely (43).

The hinge variations that we have generated could potentially alter the flexibility at the hinges and thereby the interdomain communication. Accordingly, to study the consequences of hinge variations on collective dynamics of domain motions, we modeled *M. tuberculosis* GroEL2 and the chimeras in T and R″ conformations using *E. coli* GroEL as the template, and the transition path between the two conformations for each chimera was mapped using elastic network model normal mode analysis. The intermediate deformed structures thus generated capture the topology of the

TABLE 1 Properties of the GroEL variants[a]

Hinge no.	Name of chimera	Hinge variation		Origin of GroES	Complementation	Oligomerization[b]	Prevention of aggregation
		1a or 2a	1b or 2b				
1	EAI1	::G	Δ	*M. tuberculosis*	++++	T + D	+
				E. coli	++++		
	EAI2			*M. tuberculosis*	−	T	++
				E. coli	++		
	MAI1	Δ	::EG	*M. tuberculosis*	++++	T	+++
				E. coli	++++		
	MAI2			*M. tuberculosis*	+++	T	+++
				E. coli	+++		
2	EA1	::EG	Δ	*M. tuberculosis*	−	T + D	+++
				E. coli	−		
	EA2			*M. tuberculosis*	+++	T	++
				E. coli	++		
	MA1	Δ	::VA	*M. tuberculosis*	−	T	++++
				E. coli	−		
	MA2			*M. tuberculosis*	+	T + H	+++
				E. coli	−		

[a] The abilities of the variants to complement a strain depleted of GroEL and to prevent aggregation are indicated as no ability (−), moderate abilities (+, ++, and +++), and full ability (++++).
[b] T, tetradecamer; H, heptamer; D, dimer.

conformational transitions (Fig. 6A; see also Movie S1 in the supplemental material). The domain motions in *M. tuberculosis* GroEL2 models were seen to be similar to those of *E. coli* GroEL (26, 44). An earlier study has reported rigid body movement in the apical domain resulting in a 59° twist followed by a 90° rotation along the domain axis, thereby displacing substrate binding H and L helices upwards (26, 44). Concurrently, the intermediate domain was displaced by 29° upwards.

While hinge 2 is responsible for the *en bloc* movements of the apical domain and therefore is dominated in evolution by the presence of glycine, hinge 1 is responsible for transmitting the signal and can accommodate bulkier residues (Fig. 3A). Intriguingly, replacement of the well-conserved proline at 137 by glutamic acid does not change any structural features in the models and in the crystal structure (31), suggesting that hinge 1 can tolerate variations.

Normal mode analysis of the individual mutants showed that the introduction of the point mutations at the hinges results in limited flexibility at the hinges, which correlates with constrained domain motions. This behavior is apparent in the apical-domain-exchanged chimeras. For example, insertion of Glu and Gly at hinge 2a and deletion of Val and Ala at hinge 2b in EA1 resulted in noticeable changes in the apical domain movement (Fig. 6B). Figure 6B presents a comparison of B-factors between the counter mutants as a function of residue numbers. The B-factor is a crystallographic parameter that describes the displacement of residue positions in a protein structure. The apparent reduction in the values of B-factors in the apical domain for hinge 2 variants suggests that the variations in hinge 2 are critical. However, such a variation in the B-factors is not apparent in hinge 1 mutants, suggesting that hinge 1 is more accommodative while hinge 2 is less accommodative (Fig. 6B). The analyses of low-frequency normal modes therefore suggest that the equatorial and the intermediate domains show moderate movements, while the apical domain shows large rotational and translational motions. In addition to the observed conformational transitions, normal mode analysis reveals interesting aspects pertaining to the domain motions in the chimeras. Since the apical domain undergoes large conformational changes, it is understood that the alterations in hinge 2 would severely hamper the motion of the apical domain. Normal mode analysis of the apical domain variants EA1 and EA2 revealed that B-factor fluctuations in the apical domain region are substantially reduced in EA1 owing to the mutations in hinge 2 (Fig. 6B). A similar but slightly less profound effect was observed for the variants MA1 and MA2 (Fig. 6B). While the EG insertion in EA1 leads to stearic hindrance at hinge 2a, similar insertion in MA1 at hinge 2b leads to an extra residue, thereby allowing the motion of the apical domain (Fig. 6C). Therefore, these results indicate that hinge 2 is critical for chaperone activity.

Perturbing hinge 2 has been known to result in GroEL that is defective in interactions with GroES (16). In the GroEL variants with apical domain exchange, insertions or deletion of as few as two residues at hinge 2 abolished the activity from GroEL variants, as observed for EA1 versus EA2 and MA1 versus MA2 (Fig. 2 and 3), indicating that the domain boundaries at hinge 2 are critical. Since hinges 2a and 2b are constrained during the large apical domain motions, alterations in this region pose potential steric clashes (Fig. 6). However, the equatorial-domain-exchanged variants demonstrated a distinctive behavior. Whereas variants with the GroEL2 equatorial domain EAI1 and EAI2 showed moderate activity with cognate GroES, the variants with the GroEL equatorial domain MAI1 and MAI2 showed identical activity (Fig. 2 and 4). We believe that hinge 1b, not being constrained, might be able to accommodate variations without affecting the interdomain communication and overall activity (Fig. 6A). These results, therefore, illustrate the effects of flexibility in hinge regions on the domain motion and thereafter the overall chaperonin function.

DISCUSSION

The chaperonins function by binding substrate polypeptides in an ATP-dependent manner (45). Several structural and functional studies on GroEL have established that GroEL exhibits substrate

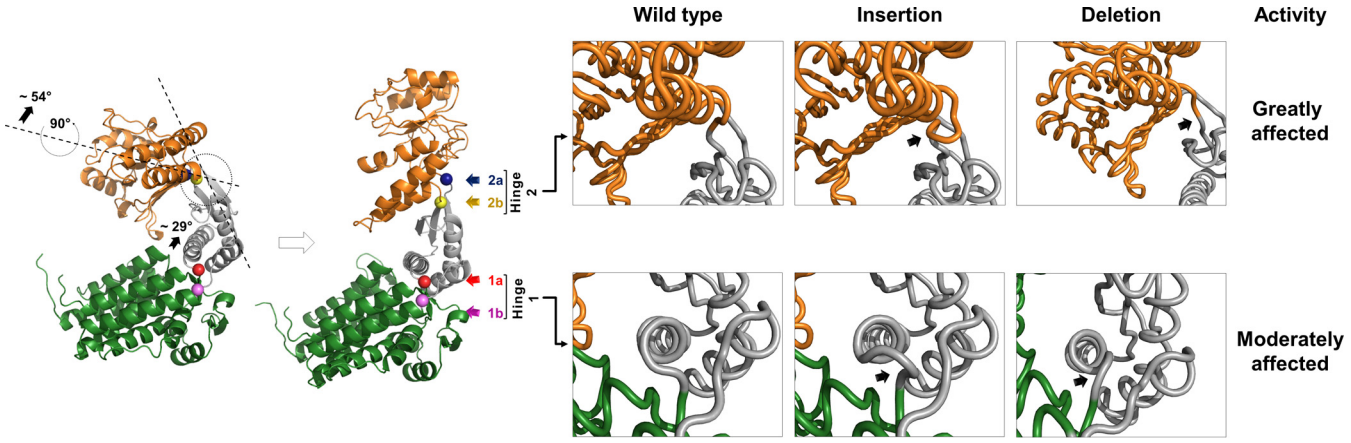

FIG 7 Effects of hinge variations on GroEL activity. Homology models of *M. tuberculosis* GroEL2 representing the T and R conformational states. The apical, intermediate, and equatorial domains are presented in gold, gray, and green, respectively, while the color-coded arrows represent the hinges. The effects of the hinge indels are compared to those of the wild type as represented. Black arrows point to the predicted structural variations at the hinges resulting from the indels. Variations at hinge 2 have been shown to greatly affect the activity.

binding rates that are determined by the bound nucleotide. ATP-bound GroEL exhibits a relaxed (R) conformation with low substrate affinity and high on/off rates, while the ADP-bound GroEL exhibits tight (T) conformation with high substrate affinity and low on/off rates. The allosteric transitions follow the concerted Monod-Wyman-Changeux (MWC) model, whereby ATP binding and hydrolysis at the equatorial domain prime the apical domain for vast conformational alterations that consequently affect substrate affinity (46–48). This crucial allosteric signal between equatorial and apical domains is efficiently transmitted by the intermediate domain via the two hinges at its extremes (Fig. 2; Table 1). Binding of ATP triggers breaking of several intra- and intersubunit salt bridges between the equatorial and intermediate domains, resulting in a 25° movement of intermediate domain through hinge 1 (18–20). This imparts strain on the salt bridges between the apical and intermediate domains, which eventually break and release the apical domain for large rotations across hinge 2 (21, 42). The hinge regions are thus critical in the GroEL mechanism, and variations in hinge sequences can potentially affect one or more features of the GroEL mechanism. In this study, domain-exchanged chimeras of *M. tuberculosis* GroEL2 and *E. coli* GroEL allowed us to probe the significance of individual hinges without influencing other features of chaperonin (Fig. 7; see also Movie S1 in the supplemental material).

The variations at hinge 2 present an interesting picture. Hinge 2 mediates large conformational changes in the apical domain, and consequently hinge 2 requires greater flexibility than hinge 1. It is likely that due to the requirement for these large conformational changes, it accommodates only smaller residues at 2a and 2b. Therefore, variations at either 2a or 2b result in severe alterations in GroEL function as observed in the apical domain chimeras (Fig. 4A and 7). Understandably, since hinge 2 does not contribute to quaternary assembly and ATP hydrolysis, mutations at hinge 2 do not affect oligomerization considerably (Fig. 5), implying that the loss of activity due to changes at hinge 2 might be due to impaired motion of the apical domain and substrate interaction. Furthermore, normal mode analysis of transitions between the two conformations of chaperonin has emphasized the significance of, and stringency at, the hinge regions. While the exposed hinge 1b moves liberally, hinge 1a remains constrained during the transition. Hinge 2, on the other hand, remains extremely constrained during the vast *en bloc* movement of the apical domain (Fig. 6 and 7).

The chimeras employed in this study allowed us to assess features of the chaperonin function, including substrate binding (Table 1). Certain chimeras were phenotypically active irrespective of weak substrate interactions. On the other hand, chimeras with apparently minor mutations at the hinges appeared to affect activity more profoundly. These results therefore demonstrate that the chaperone activity is fundamentally influenced by the interdomain communication, even if oligomerization and the ability to recognize the substrates are retained. In summary, employing genetic, biochemical, and computational platforms, we demonstrate that the hinge regions play a pivotal role in mediating these transitions to bring about the interdomain motions.

ACKNOWLEDGMENTS

We thank Stewart Cole, Arthur Horwich, NIH-NIAID Tuberculosis Vaccine Testing, Research Materials Contract (HHSN266200400091C) at Colorado State University and NBRP (NIG, Japan) (*E. coli*) for providing strains, plasmids, and antibodies. We thank T. Ramakrishna Murty and Mohan Rao for helpful discussions and support in spectroscopic studies and Gaurang Mahajan for assisting in molecular modeling.

This work was supported by a grant from the Department of Biotechnology, India (BT/PR3260/BRB/10/967/2011). N.C. was a postdoctoral fellow from the Department of Biotechnology, India. We declare no financial conflict of interest.

FUNDING INFORMATION

Department of Biotechnology, Ministry of Science and Technology (DBT) provided funding to Shekhar C. Mande under grant number BT/PR3260/BRB/10/967/2011.

REFERENCES

1. **Baneyx F, Mujacic M.** 2004. Recombinant protein folding and misfolding in *Escherichia coli*. Nat Biotechnol **22:**1399–1408. http://dx.doi.org/10.1038/nbt1029.
2. **Saibil H.** 2013. Chaperone machines for protein folding, unfolding and

disaggregation. Nat Rev Mol Cell Biol **14:**630–642. http://dx.doi.org/10.1038/nrm3658.
3. **Bukau B, Horwich AL.** 1998. The Hsp70 and Hsp60 chaperone machines. Cell **92:**351–366. http://dx.doi.org/10.1016/S0092-8674(00)80928-9.
4. **Fayet O, Ziegelhoffer T, Georgopoulos C.** 1989. The *groES* and *groEL* heat shock gene products of *Escherichia coli* are essential for bacterial growth at all temperatures. J Bacteriol **171:**1379–1385.
5. **Tilly K, Murialdo H, Georgopoulos C.** 1981. Identification of a second *Escherichia coli groE* gene whose product is necessary for bacteriophage morphogenesis. Proc Natl Acad Sci U S A **78:**1629–1633. http://dx.doi.org/10.1073/pnas.78.3.1629.
6. **Saibil H, Dong Z, Wood S, auf der Mauer A.** 1991. Binding of chaperonins. Nature **353:**25–26.
7. **Fenton WA, Horwich AL.** 1997. GroEL mediated protein folding. Protein Sci **6:**743–760.
8. **Xu Z, Horwich AL, Sigler PB.** 1997. The crystal structure of the asymmetric GroEL-GroES-$(ADP)_7$ chaperonin complex. Nature **388:**741–750. http://dx.doi.org/10.1038/41944.
9. **Bartolucci C, Lamba D, Grazulis S, Manakova E, Heumann H.** 2005. Crystal structure of wild-type chaperonin GroEL. J Mol Biol **354:**940–951. http://dx.doi.org/10.1016/j.jmb.2005.09.096.
10. **Kumar CMS, Mande SC, Mahajan G.** 2015. Multiple chaperonins in bacteria—novel functions and non-canonical behaviors. Cell Stress Chaperones **20:**555–574. http://dx.doi.org/10.1007/s12192-015-0598-8.
11. **Braig K, Otwinowski Z, Hegde R, Boisvert DC, Joachimiak A, Horwich AL, Sigler PB.** 1994. The crystal structure of the bacterial chaperonin GroEL at 2.8 Å. Nature **371:**578–586. http://dx.doi.org/10.1038/371578a0.
12. **White HE, Chen S, Roseman AM, Yifrach O, Horovitz A, Saibil HR.** 1997. Structural basis of allosteric changes in the GroEL mutant Arg197→Ala. Nat Struct Biol **4:**690–694. http://dx.doi.org/10.1038/nsb0997-690.
13. **Zeilstra-Ryalls J, Fayet O, Baird L, Georgopoulos C.** 1993. Sequence analysis and phenotypic characterization of *groEL* mutations that block λ and T4 bacteriophage growth. J Bacteriol **175:**1134–1143.
14. **Richardson A, van der Vies S, Keppel F, Taher A, Landry SJ.** 1999. Compensatory changes in GroEL/Gp31 affinity as a mechanism for allele-specific genetic interaction. J Biol Chem **274:**52–58. http://dx.doi.org/10.1074/jbc.274.1.52.
15. **Richardson A, Georgopoulos C.** 1999. Genetic analysis of bacteriophage T4-encoded cochaperone Gp31. Genetics **4:**1449–1457.
16. **Klein G, Georgopoulos C.** 2001. Identification of important amino acid residues that modulate binding of *Escherichia coli* GroEL to its various co-chaperones. Genetics **158:**507–517.
17. **Machida K, Fujiwara R, Tanaka T, Sakane I, Hongo K, Mizobata T, Kawata Y.** 2009. Gly192 at hinge 2 site in the chaperonin GroEL plays a pivotal role in the dynamic apical domain movement that leads to GroES binding and efficient encapsulation of substrate proteins. Biochim Biophys Acta **1794:**1344–1354. http://dx.doi.org/10.1016/j.bbapap.2008.12.003.
18. **Ma J, Karplus M.** 1998. The allosteric mechanism of the chaperonin GroEL: a dynamic analysis. Proc Natl Acad Sci U S A **95:**8502–8507. http://dx.doi.org/10.1073/pnas.95.15.8502.
19. **Horovitz A, Willison KR.** 2005. Allosteric regulation of chaperonins. Curr Opin Struct Biol **15:**646–651. http://dx.doi.org/10.1016/j.sbi.2005.10.001.
20. **Mizobata T, Uemura T, Isaji K, Hirayama T, Hongo K, Kawata Y.** 2011. Probing the functional mechanism of *Escherichia coli* GroEL using circular permutation. PLoS One **6:**e26462. http://dx.doi.org/10.1371/journal.pone.0026462.
21. **Kovács E, Sun Z, Liu H, Scott DJ, Karsisiotis AI, Clarke AR, Burston SG, Lund PA.** 2010. Characterisation of a GroEL single-ring mutant that supports growth of *Escherichia coli* and has GroES-dependent ATPase activity. J Mol Biol **396:**1271–1283. http://dx.doi.org/10.1016/j.jmb.2009.11.074.
22. **Horwich AL, Fenton WA.** 2009. Chaperonin-mediated protein folding: using a central cavity to kinetically assist polypeptide chain folding. Q Rev Biophys **42:**83–116. http://dx.doi.org/10.1017/S0033583509004764.
23. **Rao T, Lund P.** 2010. Differential expression of the multiple chaperonins of *Mycobacterium smegmatis*. FEMS Microbiol Lett **310:**24–31. http://dx.doi.org/10.1111/j.1574-6968.2010.02039.x.
24. **Goyal K, Qamra R, Mande SC.** 2006. Multiple gene duplication and rapid evolution in the *groEL* gene: functional implications. J Mol Evol **63:**781–787. http://dx.doi.org/10.1007/s00239-006-0037-7.
25. **Kong TH, Coates AR, Butcher PD, Hickman CJ, Shinnick TM.** 1993. Mycobacterium tuberculosis expresses two chaperonin-60 homologs. Proc Natl Acad Sci U S A **90:**2608–2612. http://dx.doi.org/10.1073/pnas.90.7.2608.
26. **Kumar CMS, Mande SC.** 2011. Protein chaperones and non-protein substrates: on substrate promiscuity of GroEL. Curr Sci **100:**1646–1653.
27. **Mande SC, Kumar CMS, Sharma A.** 2013. Evolution of bacterial chaperonin 60 paralogues and moonlighting activity, p 101–121. *In* Henderson B (ed), Heat shock proteins, vol 7. Springer, Dordrecht, Netherlands. http://dx.doi.org/10.1007/978-94-007-6787-4_7.
28. **Stewart GR, Wernisch L, Stabler R, Mangan JA, Hinds J, Laing KG, Young DB, Butcher PD.** 2002. Dissection of the heat shock response in *Mycobacterium tuberculosis* using mutants and microarrays. Microbiology **148:**3129–3138. http://dx.doi.org/10.1099/00221287-148-10-3129.
29. **Qamra R, Srinivas V, Mande SC.** 2004. *Mycobacterium tuberculosis* GroEL homologues unusually exist as lower oligomers and retain the ability to suppress aggregation of substrate proteins. J Mol Biol **342:**605–617. http://dx.doi.org/10.1016/j.jmb.2004.07.066.
30. **Kumar CMS, Khare G, Srikanth CV, Tyagi AK, Sardesai AA, Mande SC.** 2009. Facilitated oligomerization of mycobacterial GroEL: evidence for phosphorylation-mediated oligomerization. J Bacteriol **191:**6525–6538. http://dx.doi.org/10.1128/JB.00652-09.
31. **Qamra R, Mande SC.** 2004. Crystal structure of the 65-kDa heat shock protein, chaperonin 60.2 of *Mycobacterium tuberculosis*. J Bacteriol **186:**8105–8113. http://dx.doi.org/10.1128/JB.186.23.8105-8113.2004.
32. **Shahar A, Melamed-Frank M, Kashi Y, Shimon L, Adir N.** 2011. The dimeric structure of the Cpn60.2 chaperonin of *Mycobacterium tuberculosis* at 2.8 Å reveals possible modes of function. J Mol Biol **412:**192–203. http://dx.doi.org/10.1016/j.jmb.2011.07.026.
33. **Fan M, Rao T, Zacco E, Ahmed MT, Shukla A, Ojha A, Freeke J, Robinson CV, Benesch JL, Lund PA.** 2012. The unusual mycobacterial chaperonins: evidence for *in vivo* oligomerization and specialization of function. Mol Microbiol **85:**934–944. http://dx.doi.org/10.1111/j.1365-2958.2012.08150.x.
34. **Guzman LM, Belin D, Carson MJ, Beckwith J.** 1995. Tight regulation, modulation, and high-level expression by vectors containing the arabinose P_{BAD} promoter. J Bacteriol **177:**4121–4130.
35. **Horwich AL, Low KB, Fenton WA, Hirshfield IN, Furtak K.** 1993. Folding *in vivo* of bacterial cytoplasmic proteins: role of GroEL. Cell **74:**909–917. http://dx.doi.org/10.1016/0092-8674(93)90470-B.
36. **Sambrook J, Fritsch EF, Maniatis T.** 1989. Molecular cloning: a laboratory manual, 2nd ed. Cold Spring Harbor Laboratory Press, Cold Spring Harbor, NY.
37. **Warrens AN, Jones MD, Lechler RI.** 1997. Splicing by overlap extension by PCR using asymmetric amplification: an improved technique for the generation of hybrid proteins of immunological interest. Gene **186:**29–35. http://dx.doi.org/10.1016/S0378-1119(96)00674-9.
38. **Eswar N, Webb B, Marti-Renom MA, Madhusudhan MS, Eramian D, Shen MY, Pieper U, Sali A.** 2006. Comparative protein structure modeling using Modeller. Curr Protoc Bioinformatics **Chapter 5:**Unit 5.6. http://dx.doi.org/10.1002/0471250953.bi0506s15.
39. **Zheng W, Brooks BR.** 2005. Normal-modes-based prediction of protein conformational changes guided by distance constraints. Biophys J **88:**3109–3117. http://dx.doi.org/10.1529/biophysj.104.058453.
40. **Chen L, Sigler PB.** 1999. The crystal structure of a GroEL/peptide complex: plasticity as a basis for substrate diversity. Cell **99:**757–768. http://dx.doi.org/10.1016/S0092-8674(00)81673-6.
41. **Naffin-Olivos JL, Georgieva M, Goldfarb N, Madan-Lala R, Dong L, Bizzell E, Valinetz E, Brandt GS, Yu S, Shabashvili DE, Ringe D, Dunn BM, Petsko GA, Rengarajan J.** 2014. *Mycobacterium tuberculosis* Hip1 modulates macrophage responses through proteolysis of GroEL2. PLoS Pathog **10:**e1004132. http://dx.doi.org/10.1371/journal.ppat.1004132.
42. **Fei X, Yang D, LaRonde-LeBlanc N, Lorimer GH.** 2013. Crystal structure of a GroEL-ADP complex in the relaxed allosteric state at 2.7 Å resolution. Proc Natl Acad Sci U S A **110:**E2958–E2966. http://dx.doi.org/10.1073/pnas.1311996110.
43. **Chatellier J, Hill F, Foster NW, Goloubinoff P, Fersht AR.** 2000. From minichaperone to GroEL 3: properties of an active single-ring mutant of GroEL. J Mol Biol **304:**897–910. http://dx.doi.org/10.1006/jmbi.2000.4278.
44. **Ma J, Sigler PB, Xu Z, Karplus M.** 2000. A dynamic model for the allosteric mechanism of GroEL. J Mol Biol **302:**303–313. http://dx.doi.org/10.1006/jmbi.2000.4014.
45. **Hartl FU, Bracher A, Hayer-Hartl M.** 2011. Molecular chaperones in

protein folding and proteostasis. Nature **475:**324–332. http://dx.doi.org/10.1038/nature10317.
46. **Monod J, Wyman J, Changeux JP.** 1965. On the nature of allosteric transitions: a plausible model. J Mol Biol **12:**88–118. http://dx.doi.org/10.1016/S0022-2836(65)80285-6.
47. **Yifrach O, Horovitz A.** 1995. Nested cooperativity in the ATPase activity of the oligomeric chaperonin GroEL. Biochemistry **34:**5303–5308. http://dx.doi.org/10.1021/bi00016a001.
48. **Dyachenko A, Gruber R, Shimon L, Horovitz A, Sharon M.** 2013. Allosteric mechanism can be distinguished using structural mass spectrometry. Proc Natl Acad Sci U S A **110:**7235–7239. http://dx.doi.org/10.1073/pnas.1302395110.